

30+ frequencies for the δ Scuti variable 4 Canum Venaticorum: results of the 1996 multisite campaign

M. Breger¹, G. Handler¹, R. Garrido², N. Audard¹, W. Zima¹, M. Paparó³, F. Beichbuchner¹, Li Zhi-ping⁴, Jiang Shi-yang⁴, Liu Zong-li⁴, Zhou Ai-ying⁴, H. Pikall¹, A. Stankov¹, J.A. Guzik⁵, M. Sperl¹, J. Krzesinski⁶, W. Ogloza⁶, G. Pajdosz⁶, S. Zola^{6,7}, T. Thomassen⁸, J.-E. Solheim⁸, E. Serkowsch¹, P. Reegen¹, T. Rumpf¹, A. Schmalwieser¹, and M.H. Montgomery¹

¹ Astronomisches Institut der Universität Wien, Türkenschanzstrasse 17, A-1180 Wien, Austria (breger@astro.univie.ac.at)

² Instituto de Astrofísica de Andalucía, CSIC, Apdo. 3004, E-18080 Granada, Spain

³ Konkoly Observatory, Box 67, H-1525 Budapest XII, Hungary

⁴ Beijing Observatory, Academy of Sciences, Beijing, P.R. China

⁵ Los Alamos National Laboratory, XTA, MS B220, Los Alamos, NM 87545, USA

⁶ Mt. Suhora Observatory, Cracow Pedagogical University, PL-30-083 Cracow, Poland

⁷ Jagiellonian University, Ul. Orła 171 PL-30-244 Cracow, Poland

⁸ Department of Physics, University of Tromsø, N-9037 Tromsø, Norway

Received 8 April 1999 / Accepted 9 July 1999

Abstract. The evolved δ Scuti variable 4 CVn was observed photometrically for 53 nights on three continents. We found a total of 34 significant and 1 probable simultaneously excited frequencies. Of these, 16 can be identified as linear combinations of other frequencies. All significant frequencies outside the 4.5 to 10 cd^{-1} (52 to 116 μHz) range can be identified with frequency combinations, $f_i \pm f_j$, of other modes with generally high amplitudes. There exists a number of closely spaced frequencies with separations of $\sim 0.06 \text{cd}^{-1}$. This cannot be explained in terms of amplitude variability.

The results show that even for stars on and above the main sequence other than the Sun, a very large number of simultaneously excited nonradial oscillations can be detected by conventional means.

Since all pulsation modes with photometric amplitudes of 1 mmag or larger have now been detected for this star, a presently unknown mode selection mechanism must exist to select between the 1000+ of low-degree modes predicted to be excited for this (and many other) stars.

Phase differences and amplitude ratios between the y and v colors are determined for the ten main modes. The phase differences indicate p_1 to p_4 modes of $\ell = 1$ for four of these modes.

The formulae to determine the uncertainties in the amplitudes and phases of sinusoidal fits to observational data are derived in the Appendix.

Key words: stars: variables: δ Sct – stars: oscillations – stars: individual: AI CVn – stars: individual: 4 CVn

1. Introduction

The δ Scuti variables pulsate with a large number of simultaneously excited radial and nonradial modes, which makes them well-suited for asteroseismological studies. The amplitudes of the more dominant modes in the typical δ Scuti star are a few millimag, which is much higher than found in the Sun. It is now possible for ground-based telescopes to detect a large number of simultaneously excited modes with millimag amplitudes in stars other than the Sun. Because photometric studies measure the integrated light across the stellar surface, they can detect low-degree modes only. These studies require hundreds of telescope hours at observatories spread around the world in order to reduce aliasing caused by observing gaps and to lower the noise level in the power spectra.

The Delta Scuti Network (DSN) is engaged in a long-term program to determine the multifrequency structure of selected δ Scuti stars situated in different parts of the classical instability strip. These stars include 4 CVn (cool, evolved), BI CMi (cool, less evolved), FG Vir (center), XX Pyx (hot, unevolved) and θ^2 Tau (hot, evolved).

The star 4 CVn is of particular interest for a number of reasons: (i) The star is highly evolved ($\log g = 3.5 \pm 0.1$ at $T_{\text{eff}} = 6900 \pm 100\text{K}$) for a δ Scuti variable and is on its way to the giant branch. For these stars, a very dense forest of excited modes is predicted (Dziembowski & Krolikowska 1990). (ii) The star exhibits amplitude variability with a typical time scale of years, but some rapid changes are also known. An example is the rapid change of the amplitude of the 7.38cd^{-1} mode between 1974 and 1976. (iii) The amplitude variability may be connected with transferring power between different modes through resonances. In this respect, a study of combination frequencies, $f_i \pm f_j$, is important.

Table 1. Journal of photoelectric measurements of 4CVn

Start HJD	Length hours	Obs.	Start HJD	Length hours	Obs.
116.71	6.39	McD	153.09	6.43	XL
117.88	3.97	McD	154.39	1.91	SNO
118.73	7.68	McD	154.65	8.97	McD
119.70	8.31	McD	155.65	8.86	McD
120.48	1.46	Suh	157.64	9.16	McD
121.71	8.08	McD	158.64	9.10	McD
122.73	7.62	McD	159.11	5.19	XL
123.48	2.49	Suh	159.36	4.29	Skib
123.81	5.47	McD	159.64	9.34	McD
127.72	7.62	McD	160.17	4.60	McD
128.68	6.60	McD	160.34	9.21	SNO
139.47	4.83	Pisz	161.01	8.18	XL
140.32	8.12	Pisz	161.35	5.93	Suh
141.35	6.01	Pisz	161.57	1.55	SNO
142.32	8.24	Pisz	162.48	5.76	SNO
143.21	3.73	XL	162.69	7.76	McD
144.14	5.77	XL	163.64	8.91	McD
145.12	6.54	XL	164.34	5.46	SNO
146.21	4.07	XL	164.80	2.81	McD
147.66	5.11	McD	165.93	2.00	McD
151.09	6.93	XL	168.69	6.22	McD
151.40	5.89	Pisz	170.33	7.34	SNO
151.68	8.26	McD	170.66	6.24	McD
152.09	7.40	XL	171.35	5.82	SNO
152.33	7.34	Skib	171.38	3.29	Suh
152.33	5.28	Pisz	171.88	2.60	McD
152.63	8.78	McD			

McD: McDonald, Suh: Suhora, Pisz: Piskésető
 XL: Xing Long, Ski: Skibotn, SNO: Sierra Nevada

The variability of 4 CVn (HR 4715 = HD 107904 = AI CVn, F3III–IV) was discovered by Jones & Haslam (1966). Subsequent period determinations based on observations of only a few nights each led to a large number of reported periods and solutions, usually in disagreement with each other. Extensive unpublished single-site photometry by Fitch and coworkers (Fitch 1980) showed the multiperiodicity, but did not present a consistent picture of this complex variability. The multisite campaign of the Delta Scuti Network carried out in 1983 and 1984 (Breger et al. 1990, hereafter called Paper I) revealed five frequencies of pulsation. A subsequent analysis of the previous published and unpublished data extended the number of frequencies to 7 and showed that the complex behavior of 4 CVn was caused by amplitude variability of pulsation modes with essentially constant frequencies (Breger 1990a, Paper II). A photometric study undertaken with the Vienna Automatic Photoelectric Telescope (APT) in Arizona covering 204 hours increased the number of detected frequencies to 19 (Breger & Hiesberger 1999, Paper III). 6 of the 19 were combination frequencies.

The present paper reports the results of a multisite photometric campaign carried out by the Delta Scuti Network on three continents and the considerable increase in the number of pulsation modes detected in 4 CVn.

2. New measurements

During 1996 February and March, 4 CVn was observed photoelectrically together with two comparison stars for 53 nights (325 hours) at six observatories. The following telescopes were used: McDonald Observatory 0.9m (observers Handler, Audard); Xing Long, China, 0.85m (observer Li Zhiping); Sierra Nevada Observatory, Spain, 0.9m (observers Garrido, Beichbuchner); Piskésető, Hungary, 0.5m (observers Páparó, Pikall, Stankov, Zima); Mt. Suhora, Poland, 0.6m (observers Ogloza, Pajdosz, Zola); and Skibotn, Norway, 0.5m (observer Thomassen). The dates of observation can be found in Table 1.

The three-star technique, in which measurements of the variable star are alternated with those of two comparison stars, was adopted. With the three-star technique adopted by the Delta Scuti Network, the required high photometric accuracy is achieved by alternating measurements of the variable star with those of two carefully chosen comparison stars. The same photometric channel is used for all three measurements. The procedure can produce the required long-term stability of 2 mmag or better (also within different observatories), but yields a variable-star measurement only every five minutes. The technique works well for periods between 30 minutes and several days and has been described by Breger (1993).

The two comparison stars, HR 4843 (F6IV) and HR 4728 (G9III), have been used before as comparison stars. No evidence for any variability has been found. At McDonald and Sierra Nevada Observatories the measurements were made through the Stromgren v and y filters to provide a relatively large baseline in wavelength. The large baseline is needed to determine reliable phase differences (see Sect. 4) and cannot be achieved with the b filter. The u filter was also not chosen because of the very large potential for systematic observational errors. At the other observatories, only the Johnson V filter was used, which has the same effective wavelength as the Stromgren y filter.

The resulting light curves are shown in Fig. 1, where the observations can also be compared with the fit to be derived in the next section.

3. Detection of the pulsation frequencies

The pulsation frequency analyses were performed with a package of computer programs with single-frequency and multiple-frequency techniques (programs PERIOD, Breger 1990b; PERIOD98, Sperl 1998), which utilize Fourier as well as multiple-least-squares algorithms. The latter technique fits a number of simultaneous sinusoidal variations in the magnitude domain and does not rely on prewhitening. For the purposes of presentation, however, prewhitening is required if the low-amplitude modes are to be seen. Therefore, the various power spectra are presented as a series of panels, each with additional frequencies removed relative to the panel above.

One of the most important questions in the examination of multiperiodicity concerns the decision as to which of the detected peaks in the power spectrum can be regarded as variability intrinsic to the star. Due to the presence of nonrandom errors in photometric observations and because of observing gaps, the

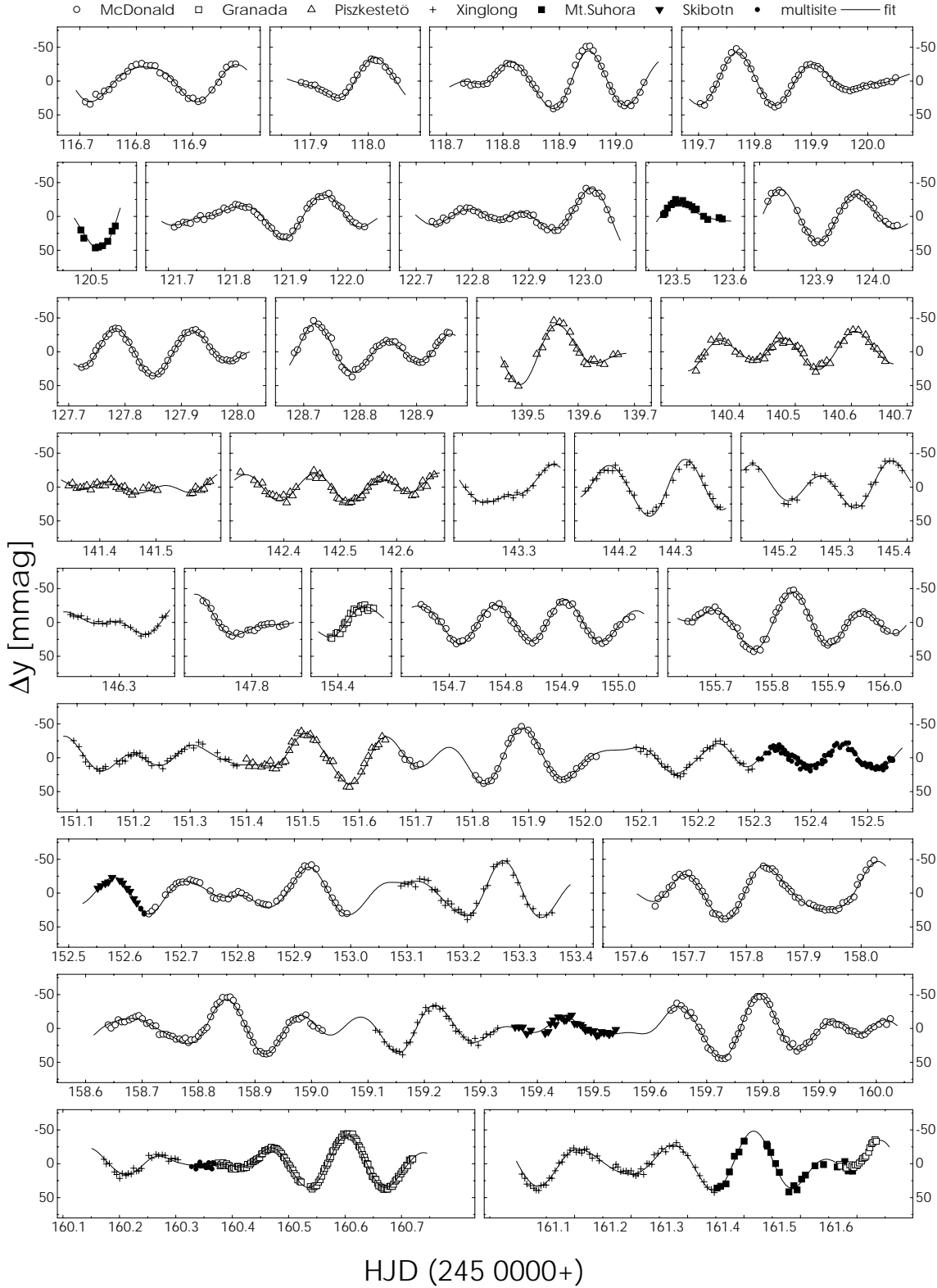


Fig. 1. Multisite photoelectric three-star-photometry of 4 CVn obtained during the 1996 DSN campaign. Δy and Δv are the observed magnitude differences (variable – comparison stars) normalized to zero in the narrowband *uvby* system. The fit of the 34-frequency solution derived in this paper is shown as a solid curve. Note the excellent agreement between the measurements and the fit

predictions of standard statistical false-alarm tests give answers which we consider to be overly optimistic. In a previous pa-

per (Breger et al. 1993) we argued that a ratio of amplitude signal/noise = 4.0 provides a useful criterion for judging the re-

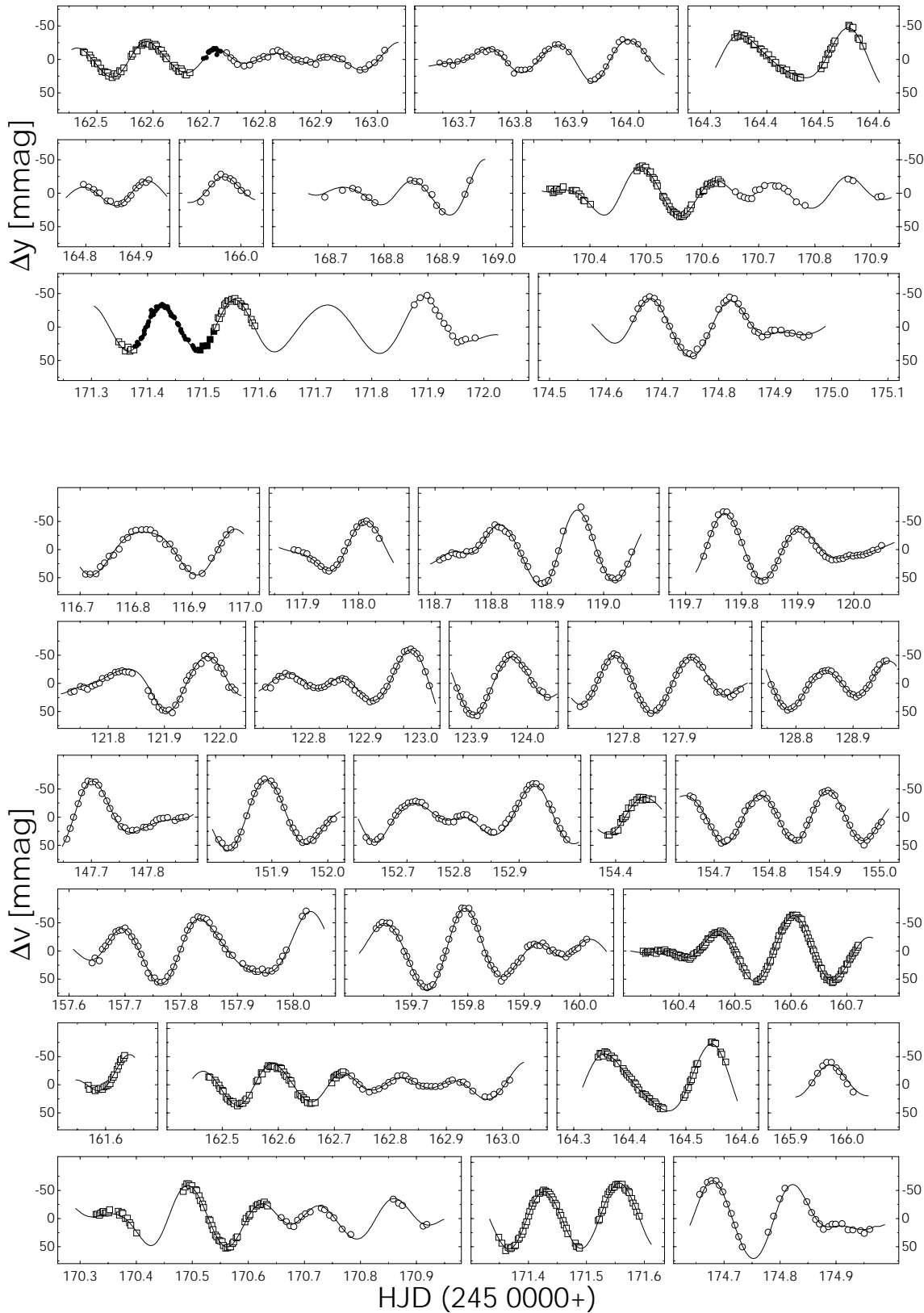


Fig. 1. (continued)

ality of a peak. This empirically determined limit now has some theoretical underpinning (Kuschnig et al. 1997).

For peaks at harmonics or combination frequencies, we must relax the criterion. The reason is the statistically different ques-

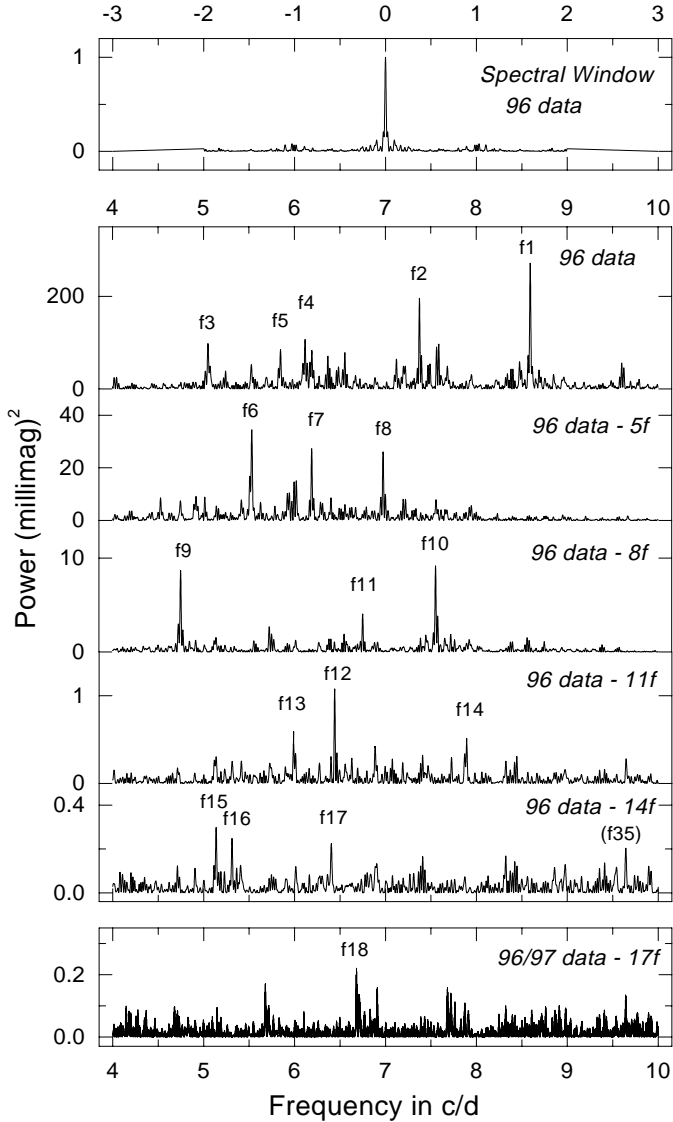


Fig. 2. Power spectrum of 4 CVn in the 4 to 10 cd^{-1} range, where the main pulsation frequencies are situated. The spectra based on the 1996 v and y data are shown before and after applying multiple frequency solutions. See text for the numbering scheme and a discussion of significance levels

tion asked. In a general search we must consider the occurrence of even a single accidental peak among a large number of possible frequencies from 0 to the Nyquist frequency, f_n . For known frequency values (such as combination frequencies), we only have to consider the possibility of an accidental peak occurring in a narrow frequency range near the expected combination frequency. In the following paragraph, we provide a rough estimate of the significance criterion for combination frequencies which should have the same false alarm probability as the 4.0 criterion does for the identification of general frequencies.

For the present case, using the first 18 frequencies we have $18^2 = 324$ potential combination peaks, and in the neighborhood of each expected peak we examine a frequency range of length $2\sqrt{2}\sigma = 0.0028 \text{ cd}^{-1}$ ($\sigma = 0.001 \text{ cd}^{-1}$ is taken to be a

representative error bar for frequencies determined in the 1996 campaign). We are thus examining a total frequency range of $324 \cdot 0.0028 \text{ cd}^{-1} = 0.907 \text{ cd}^{-1}$. According to Scargle (1982), the significance level z_0 (signal to noise ratio in *power*) for detection scales like

$$z_0 = \text{const.} + \ln(N),$$

where N is the number of independent frequencies searched. Clearly, N is proportional to the frequency range considered, so for a subset Δf of the total frequency range we can write

$$z_0 = 12.57 + \ln(\Delta f / f_n),$$

where $f_n \approx 120 \text{ cd}^{-1}$ is the Nyquist frequency; for $\Delta f = f_n$, we have $z_0 = 12.57$, where the value of this constant has been chosen so as to yield our empirically chosen cutoff of 4.0 when translated back into amplitude ($2\sqrt{z_0/\pi} = 4.0$). If we instead set $\Delta f = 0.907 \text{ cd}^{-1}$, in order to search for combination frequencies, we find $z_0 \approx 7.7$, which implies a signal to noise in amplitude of ≈ 3.1 . For the present analysis, we have chosen to use the more conservative value of 3.5 for our significance criterion; various tests with the present data set involving randomly selected frequency combinations suggest that this value provides a very strict detection criterion.

The amplitude signal/noise values listed in Table 2 refer to formally computed values from the combined y and v data set. Because of slight phase shifts between different colors, the true detection significance is probably higher, e.g. a phase shift of 6.5 degrees between y and v leads to an underestimate of the shifted amplitude of 7.2% of its value. For the modes with possible amplitude variability, the S/N values of the detection were computed from the combined 1996/7 data sets and are shown in italics. The noise was calculated by averaging the amplitudes (oversampled by a factor of 20) over 3 cd^{-1} regions centered around the frequency under consideration. In the low-frequency 0–4 cd^{-1} range, the value from 0.5 to 4 cd^{-1} was computed. These fairly large frequency regions make the detection criterion relatively insensitive to isolated peaks in the power spectrum.

For the frequency detection, we combined the y (2164 measurements) and v data (1185 measurements). The dependence of the pulsation amplitude on wavelength was compensated by multiplying the v data set by an experimentally determined factor of 0.66. This scaling also offsets the higher noise level of the v data in the frequency region under consideration. After the 1996 data were analyzed up to the noise level, the analysis was repeated by adding the measurements from 1997 (Paper III) and weighting according to the length of coverage (1996: 335 hours, 1997: 204 hours). This allowed the detection and confirmation of the pulsation modes with variable amplitudes between the two years. Furthermore, the increased time base made it possible to determine more accurate frequency values, which may, however be afflicted by annual aliasing of $\pm 0.0026 \text{ cd}^{-1}$.

Note that different colors and data sets were only combined to detect the frequencies and to determine the significance of the detection. The amplitudes listed in Table 2 were calculated with separate solutions for each color. If we assume completely random photometric errors, the expected uncertainties in the

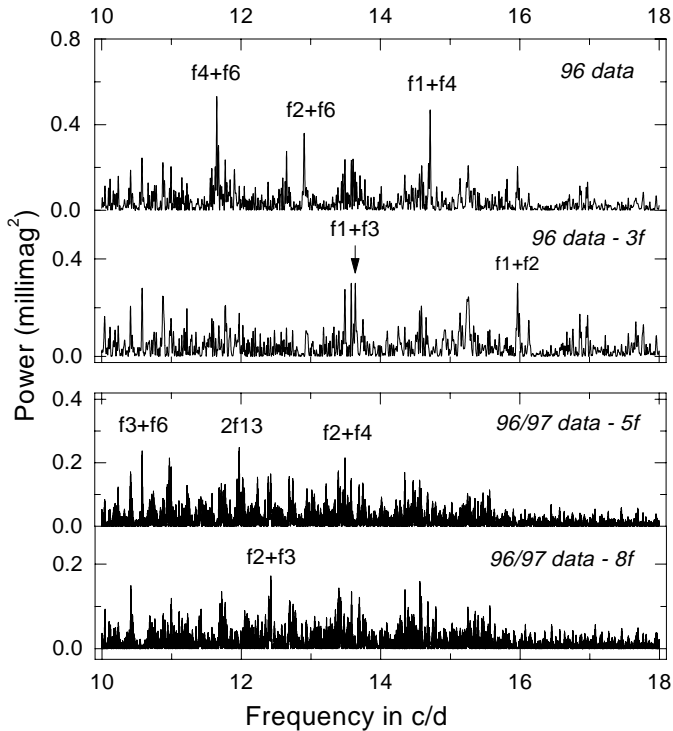


Fig. 3. Power spectrum of 4 CVn in the high-frequency range. The highest nine peaks can be matched exactly by expected combination frequencies, f_i+f_j

values of the derived amplitudes can be calculated from the residuals of the two photometric data sets. The equation used and the derivation is shown in the Appendix. The uncertainties ~ 0.1 mmag are shown in Table 2.

Anticipating the results, we divide the frequency spectrum into three separate regions based on the nature of the peaks in the power spectrum.

3.1. The main pulsation frequencies

The main pulsation frequencies of 4 CVn are found in the region of 4 to 10 cd^{-1} . Fig. 2 and Table 2 show the results of the multiperiod analysis: 18 statistically significant and one additional promising peak are found. All modes with photometric amplitudes ~ 1 mmag or larger have been detected. A formal limit of 0.5 mmag, corresponding to an amplitude signal/noise limit of 4.0, is derived. The power spectrum of the residuals suggests that additional modes with small amplitudes are excited as well.

An interesting feature of the results concerns a number of closely spaced frequencies: 6.190 and 6.117 cd^{-1} , 6.750 and 6.680 cd^{-1} (see below), and 6.440 and 6.404 cd^{-1} . Before one accepts these detected frequencies as separate pulsation modes, one needs to eliminate the possibility of a single frequency with amplitude variability. Such numerical tests are included in the reduction packages, PERDET and PERIOD98, used in the present investigation. These tests show that such a single-frequency fit with a variable amplitude cannot reproduce the observed behavior.

3.2. The high-frequency region: Combination frequencies

We now turn to the frequency range above 10 cd^{-1} . Fig. 3 shows the existence of a number of peaks in the 1996 data, which was analyzed in the same manner as for the 4–10 cd^{-1} range. The five main peaks can be immediately identified with combination frequencies, f_i+f_j . The agreement cannot be accidental since the values of these expected frequencies are quite accurate to ± 0.001 cd^{-1} . Four of these five peaks were already known from the analysis of the 1997 APT data (Paper III).

The 1996 data also show additional promising peaks. Some of these peaks become statistically significant once the 1997 data are included in the analysis. Altogether we find eight combination frequencies.

The peak at 11.9729 cd^{-1} , which has higher amplitude in the 1997 than in the 1996 data, may be related to f_{13} at 5.98647 cd^{-1} . The formal multifrequency solution indicates a frequency ratio of 1.99999. This indicates exact doubling if the uncertainties in the frequency determinations are considered. The probability of an accidental agreement is small. In principle, a frequency match with f_4+f_5 , which occurs at 11.9674 cd^{-1} , is also possible, although the frequency resolution of the combined 1996/7 data may exclude this. Since f_4+f_5 only has about half the power of the $2 \cdot f_{13}$ identification, we regard the $2 \cdot f_{13}$ identification as the more probable one.

The existence of a $2f$ term is not unusual in variable stars of large amplitude and indicates a light curve which is not strictly sinusoidal. While this usually occurs for modes of high amplitude, the observed photometric amplitude of f_{13} is very small (~ 1 mmag). It is possible to argue that f_{13} is an $\ell = 3$ or 4 mode with a large physical amplitude, which only appears small due to a large geometric reduction factor. Using formulae given in Dziembowski (1977), we find, for models appropriate to 4 CVn, that an $\ell = 3$ mode would have in general only about 10% the observed amplitude of an $\ell = 1$ mode, if both modes are assumed to have the same physical amplitude. In principle, f_{13} could therefore be a high-amplitude, intermediate- ℓ mode, for which nonlinear distortion effects could produce a $2f$ term. In this case, the surface flux perturbations associated with the harmonic would not (for $\ell \neq 0$) have the same spherical harmonic structure as the original mode, and thus might well experience less geometrical cancellation (Brassard et al. 1995). However, this explanation is somewhat contrived. Another perhaps more plausible explanation is simply a resonance: due to a resonance, f_{13} excites another p-mode at exactly twice its frequency value.

3.3. The low-frequency region: Combination frequencies

In the frequency region of 0 to 4 cd^{-1} we expect to find g modes as well as combinations of the pulsation modes, f_i-f_j . This is also the region in which the observational uncertainties may become larger, both due to the $1/f$ dependence of atmospheric effects as well as residual extinction and zero-point difficulties.

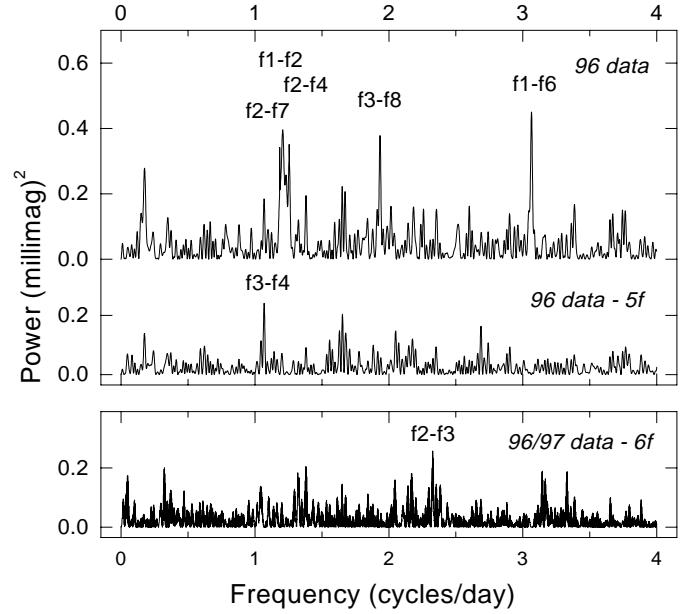
The results at low frequencies are similar to those at high frequencies: the dominant peaks are combination frequencies. Fig. 4 shows that the six dominant peaks can be identified with

Table 2. The frequency spectrum of 4 CVn in 1996

Frequency cd^{-1}	Amplitude $\mu\text{Hz}/\text{ID}$	Amplitude 1996		Significance Ampl. S/N
		y filter mmag	v Filter mmag	
Significant frequencies ± 0.09 ± 0.11				
f_1 , 8.595	99.48	15.3	22.9	118
f_2 , 7.375	85.36	11.6	17.4	96
f_3 , 5.048	58.42	10.7	16.4	95
f_4 , 6.117	70.80	9.2	14.3	83
f_5 , 5.851	67.72	10.1	15.0	90
f_6 , 5.532	64.03	6.4	10.1	57
f_7 , 6.190	71.64	5.7	8.1	51
f_8 , 6.976	80.75	5.0	7.4	45
f_9 , 4.749	54.96	3.2	4.9	27
f_{10} , 7.552	87.41	3.3	4.9	26
f_{11} , 6.750	78.13	0.9	1.6	9
f_{12} , 6.440	74.54	1.6	2.4	14
f_{13} , 5.986	69.29	0.8	1.4	7.7
f_{14} , 7.896	91.39	0.8	0.9	6.6
f_{15} , 5.134	59.42	0.8	1.1	6.8
f_{16} , 5.314	61.51	0.8	1.0	5.8
f_{17} , 6.404	74.12	0.4	1.3	5.1
f_{18} , 6.680	77.32	0.2	0.5	5.1
f_{19} , 11.649	$= f_4 + f_6$	0.7	1.4	6.2
f_{20} , 14.712	$= f_1 + f_4$	0.7	1.0	5.4
f_{21} , 12.907	$= f_2 + f_6$	0.4	0.5	4.1
f_{22} , 15.970	$= f_1 + f_2$	0.6	0.7	4.2
f_{23} , 13.643	$= f_1 + f_3$	0.5	0.6	3.6
f_{24} , 10.580	$= f_3 + f_6$	0.6	0.8	4.4
f_{25} , 11.973	$= 2f_{13}$	0.4	0.5	4.1
f_{26} , 13.492	$= f_2 + f_4$	0.5	0.6	3.6
f_{27} , 12.423	$= f_2 + f_3$	0.3	0.3	3.7
f_{28} , 3.063	$= f_1 - f_6$	0.6	0.9	4.6
f_{29} , 1.069	$= f_4 - f_3$	0.5	1.0	4.4
f_{30} , 2.327	$= f_2 - f_3$	0.2	0.4	4.2
f_{31} , 1.258	$= f_2 - f_4$	0.6	0.5	4.0
f_{32} , 1.929	$= f_8 - f_3$	0.5	0.5	3.9
f_{33} , 1.185	$= f_2 - f_7$	0.3	0.5	3.8
f_{34} , 1.220	$= f_1 - f_2$	0.5	0.5	3.5
Probable frequencies				
f_{35} , 9.645	111.63	0.6	0.6	3.8
Residuals, single msmt.				
		3.0	2.7	

known values from combination frequencies. The matches are exact. A seventh frequency at $2.327 \text{ cd}^{-1} = f_2 - f_3$, previously found in the 1997 data (Paper III), had very small amplitudes during 1996. More details can be found in Table 2.

Near 1.2 cd^{-1} a triple peak is found and three closely spaced combination modes can be identified. The detection of the three modes is significant and should be correct. However, due to the frequency separation of only $\sim 0.04 \text{ cd}^{-1}$, the amplitudes of those three modes listed in Table 2 may be uncertain. Such an uncertainty in the v amplitude also exists for the f_{29} at 1.069 cd^{-1} due to the closeness of the frequency to 1 cd^{-1} and the relatively small data set.

**Fig. 4.** Power spectrum of 4 CVn for the low-frequency range. The seven highest and significant peaks can be identified with mode combinations, $f_i - f_j$ **Table 3.** Phase differences of 4 CVn

Frequency cd^{-1}	Amplitude ratio v/y	Phase differences in degrees $\phi_v - \phi_y$	
f_1	8.595	1.492 ± 0.007	-2.0 ± 0.3
f_2	7.375	1.508 ± 0.010	-2.3 ± 0.4
f_3	5.048	1.530 ± 0.011	-1.9 ± 0.4
f_4	6.117	1.534 ± 0.012	-4.5 ± 0.5
f_5	5.851	1.484 ± 0.012	-6.8 ± 0.4
f_6	5.532	1.61 ± 0.02	-4.8 ± 0.8
f_7	6.190	1.49 ± 0.02	-2.0 ± 0.8
f_8	6.976	1.50 ± 0.02	$+1.2 \pm 0.9$
f_9	4.749	1.61 ± 0.04	-1.3 ± 1.6
f_{10}	7.552	1.43 ± 0.03	-5.1 ± 1.1

We note that the pulsation frequencies involved in the detectable combinations, $f_i - f_j$, are those with high amplitudes. We will return to a more detailed analysis of which modes form interactions and the possible time variability of these components in a later section.

We note that all pulsation modes with photometric amplitudes of 1 mmag or larger excited during the years 1996 and 1997, should have been detected for this star. However, theoretical modelling has predicted the presence of 1000+ of unstable low-degree modes predicted to be excited in 4 CVn (Dziembowski 1997). Since the number of detected modes is relatively small, a presently unknown mode selection mechanism must exist to select between these modes.

3.4. Comparison between the 1996 and 1997 results

The multisite campaign reported in this paper was more extensive than the single-site set observations carried out during 1997

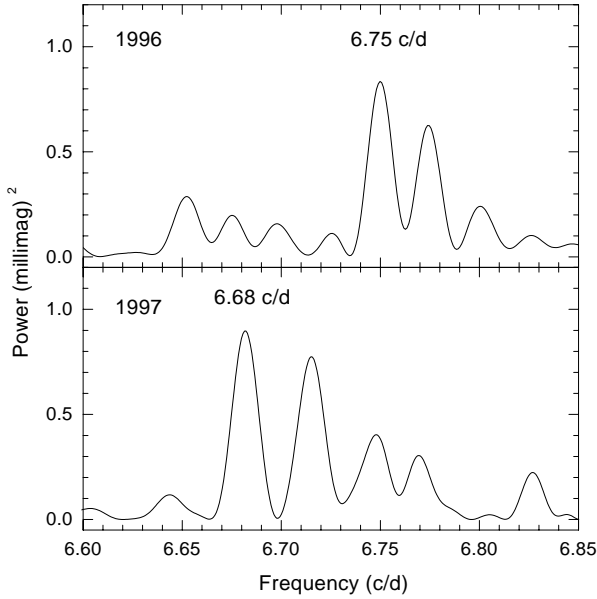


Fig. 5. The change of the modes around 6.7 cd^{-1} between 1996 and 1997. The power spectrum of the residuals after multifrequency solutions without the two modes near 6.7 cd^{-1} are shown. The width of the individual peaks also indicates that the 6.68 and 6.75 cd^{-1} peaks cannot be the same peak affected by insufficient frequency resolution

using the APT. Consequently, the number of frequencies discovered could be extended considerably: from 19 to 34. For most detected modes, the results for the two years are in excellent agreement with each other. This verifies that the significance criterion leads to reliable results.

The amplitudes of the different modes found for 1996 and 1997 also are very similar and generally within the precision limits of determining these amplitudes. This is not surprising, since the amplitude variability of 4 CVn generally occurs with time scales of 10 years or more (Paper II).

We will now discuss a few interesting modes for which the results differed for the two years:

(i) For 1996 a frequency at 6.75 cd^{-1} was found, free of 1 cd^{-1} aliasing. The 1997 data showed a value of 6.68 cd^{-1} (or $5.68, 7.68 \text{ cd}^{-1}$). Could these two peaks correspond to the same mode? The frequency resolution for the two years is considerably higher than the separation of the two peaks. In order to examine the separation in more detail, we computed full multifrequency solutions without these two modes for both years. This method discriminates against these two modes since aliasing causes some power to be picked up by other pulsation modes. Nevertheless, both modes were still present. This is demonstrated in Fig. 5, which shows the power spectra in this region for the two years. We have also tested the hypothesis that an unknown phenomenon causes the frequency to drift by 0.07 cd^{-1} in one year. The data sets cover 58 and 69 days, respectively. Such a frequency drift should be visible within the two data sets. No frequency drift was found. Note that the precision of the measurements is insufficient to detect amplitude drifts of a few tenths of a millimag within the annual data. We conclude

that the two modes are real and show amplitude variability between 1996 and 1997.

(ii) The amplitude of the dominant mode of pulsation, f_1 , increased by 12% from 1996 to 1997 (12.3% in y , 12.6% in v : the difference between the two colors is not significant). This small change is not unusual and was also observed in the time period 1974–1978 (Paper II).

(iii) The amplitudes of the combination frequencies can also be variable. The best example is provided by the pair, f_2+f_3 and f_2-f_3 . Both combinations increased from the level of detectability in 1996 to about 1 mmag in 1997. The fact that both varied similarly argues in favor of an astrophysical, rather than observational, origin. It is a fascinating speculation that the behavior may be related to the fact that f_2 is one of the modes with the most rapid amplitude variability.

4. Phase differences and amplitude ratios between v and y

The study of asteroseismology requires detailed pulsation mode identifications: the pulsational quantum numbers (n, ℓ, m) need to be determined. One of several promising methods uses the sizes of the observed phase differences between the light curves at different wavelength (e. g. Watson 1988, Garrido et al. 1990), since the sizes of the phase differences are a function of ℓ . The method has been applied successfully before (e. g. the star FG Vir, Breger et al. 1999). The application to 4 CVn requires accurate observational determinations as well as detailed model calculations. While the theoretical modelling is the subject of a later paper, here we can derive the measured values. We note that high photometric precision is needed to determine these reliably.

Due to a number of potential sources of error, the determination of the phase differences from the observational data is not straightforward. In order to avoid systematic errors caused by the (small) amplitude variability between 1996 and 1997, separate multifrequency solutions need to be made for the two years. This leads to a large number of degrees of freedom associated with 34 frequencies and 4 data sets (two colors each for 1996 and 1997). While the mode detections are statistically significant, for most modes with small amplitudes, the derived phase differences between v and y are not meaningful. In fact, only for the ten modes with the highest amplitudes do we regard the differences as significant.

A preliminary analysis indicated an average amplitude ratio of $v/y = 1.51$ and phase differences, $\phi_v - \phi_y$, near zero. This suggests how the number of degrees of freedom can be reduced: for the many modes with small amplitudes, f_{11} to f_{34} , an amplitude ratio of 1.51 and zero phase difference were assumed. For the ten modes with relatively large amplitudes, the phase differences and amplitude ratios were computed and shown in Table 3. Numerical simulations with different noise levels confirmed that this conservative approach is reasonable.

The expected uncertainties in the values of the derived phase differences and amplitude ratios can now be calculated from the residuals of the four photometric data sets. For the 1996 data, the observational details have been discussed in the previous

section. For the 1997 APT data we find formal values of amplitude uncertainties, $\sigma(a)$, of 0.074 mmag in y and 0.079 in v (see the Appendix for the equations). Finally, the statistical uncertainties of the amplitude ratios and phase differences were computed with standard error propagation relations and are listed in Table 3. We note again that these values are the formal uncertainties based on the assumption of random observational noise with no correlation between the four different data sets. Two deviations from the assumption likely to be present are the similar noise behavior of the two colors obtained almost simultaneously and the effect of unresolved additional frequencies. Both effects would cause us to *overestimate* the size of the true errors.

The application of the derived phase differences for mode identifications is beyond the scope of this paper and requires the computation of specific pulsation models, which has only been started at this time. However, some important, tantalizing observation can already be made: Four frequencies (f_3 , f_7 , f_2 and f_1) show essentially identical phase differences near -2.1 degrees. The spacings of these frequencies are 1.14, 1.18 and 1.22 cd^{-1} , respectively, which correspond to adjacent radial orders for 4 CVn. Preliminary calculations indicate p_1 , p_2 , p_3 and p_4 modes of $\ell = 1$.

5. Combination frequencies

The present study has detected a large number of combination frequencies in both the low- and high-frequency domains. The modes involved in the combinations are those with high amplitudes. A scaling of the amplitudes involved indicates that the low-amplitude modes could also be coupled, but would lead to combination amplitudes too small to be detected. There does not exist a one-to-one relationship between the amplitudes of the combination and the main frequencies involved in the combinations. This is not surprising because the measured photometric amplitudes refer to the integrated brightness change across the stellar disk and not the true pulsational amplitude. Since the combination frequencies may have a different angular dependence than the parent modes (e.g. see Dziembowski 1982), they will experience a different amount of geometric cancellation.

As shown in Garrido & Rodriguez (1996), it is possible to estimate phases and amplitudes of the combination terms in a high-amplitude radially pulsating star. The method takes into account the information contained in the harmonic series to predict the combinations terms. The analysis for 4 CVn shows no harmonic high enough to be significant, except for the exceptional case of f13. It could be interesting to apply the results found for the radial modes of SX Phe by Garrido & Rodriguez to this star in order to confirm the nonradial nature of the modes exhibited by 4 CVn. A detailed comparison will be the subject of the next paper on this star.

The following modes were most often involved in forming combinations with detectable amplitudes: f_2 and f_3 (each 7 times), f_1 and f_4 (each 5 times) and f_6 (4 times). Note that no combination frequencies were detected for f_5 , which also shows a high amplitude in integrated light. Other interesting properties are:

(i) The amplitudes of the combination frequencies can vary strongly from year to year. This is not accompanied by large amplitude variations of the main pulsation modes involved in the combination frequencies. An example is the combinations of f_2 and f_3 , which changed their amplitudes by more than a factor of 3 between 1996 and 1997. The fact that both f_2+f_3 and f_2-f_3 changed similarly argues against a possible explanation in terms of observational errors.

(ii) The amplitudes of f_i+f_j and f_i-f_j are often, but not always, similar in size. An example is provided by the peak at $11.649 \text{ cd}^{-1}=f_4+f_6$, which is the most dominant combination frequency found in this study. The corresponding peak in the power spectrum of f_4-f_6 is not seen, although it should have been easily detected.

(iii) The present study has detected about twice as many sums of frequencies as differences. This result is probably an observational artifact because of the lower observational noise at high frequencies.

Acknowledgements. It is a pleasure to thank Alosha Pamyatnykh and Paul Bradley for stimulating discussions. This investigation has been supported by the Austrian Fonds zur Förderung der wissenschaftlichen Forschung, project number S7304. The observers were partially supported by the following grants: Polish National Committee for Scientific Research Grant 2-2109-91-02, the Chinese National Natural Science Foundation, Hungarian research grant OTKA No. T02528, and NASA Astrophysics Theory grant S-398340-F.

Appendix A: derivation of the uncertainties in the amplitude and phase in photometric data

Suppose we have N measurements of the magnitudes, m_i , at times t_i . We assume that the times of the observations are error free, but that the brightness measurements m_i are subject to random errors, Δm_i , which have an average of zero, a constant root-mean-square amplitude, and are not correlated in time. Mathematically, we write these conditions as

$$\begin{aligned} \langle \Delta m_i \rangle &= 0, \\ \langle \Delta m_i \Delta m_j \rangle &= \langle (\Delta m_i)^2 \rangle \delta_{ij} \\ &= \sigma^2(m) \delta_{ij}, \end{aligned} \quad (\text{A1})$$

where the brackets $\langle \rangle$ denote a statistical average, and δ_{ij} is the Kronecker δ , which is equal to 1 if $i = j$ and is 0 otherwise.

In order to analyze our time series data, we wish to fit a sinusoid to it. Specifically, we fit the function

$$f(t) = a_0 + a \sin(\omega t_i + \phi), \quad (\text{A2})$$

where for the purposes of this derivation the frequency ω is assumed to be known, but where the amplitude a and phase ϕ are yet to be determined; this situation is encountered, for example, if one has data from previous observations which tightly constrain a known frequency, and one wishes to solve for the amplitude and phase of the signal in the current data set. The parameter a_0 represents a constant offset, and can be related to the mean value of the signal, as we show below. We define

$$\begin{aligned}\chi^2 &\equiv \sum_{i=1}^N [m_i - f(t_i)]^2 \\ &= \sum_{i=1}^N [m_i - a_0 - a \sin(\omega t_i + \phi)]^2,\end{aligned}\quad (\text{A3})$$

where the minimum in χ^2 corresponds to the best fit solution of the model parameters.

Minimizing χ^2 with respect to a_0 , a , and ϕ , we obtain the following three relations:

$$\frac{\partial \chi^2}{\partial a_0} = 0 \Rightarrow a_0 = \frac{1}{N} \sum_{i=1}^N m_i \quad (\text{A4})$$

$$\frac{\partial \chi^2}{\partial a} = 0 \Rightarrow a = \frac{2}{N} \sum_{i=1}^N m_i \sin(\omega t_i + \phi) \quad (\text{A5})$$

$$\frac{\partial \chi^2}{\partial \phi} = 0 \Rightarrow 0 = \sum_{i=1}^N m_i \cos(\omega t_i + \phi), \quad (\text{A6})$$

where we have assumed that the time series is of such a length that the relations $\sum_{i=1}^N \sin^2(\omega t_i + \phi) = N/2$ and $\sum_{i=1}^N \sin(\omega t_i + \phi) \cos(\omega t_i + \phi) = 0$ are valid.

In general, the random errors in magnitude, Δm_i , produce small variations in the fit parameters (Δa , $\Delta \phi$) from their “true” values. If we take a total differential of Eq. A5 with respect to (m_i, a, ϕ) , then we obtain

$$\begin{aligned}\Delta a &= \frac{2}{N} \sum_{i=1}^N [\Delta m_i \sin(\omega t_i + \phi) + m_i \cos(\omega t_i + \phi) \Delta \phi] \\ &= \frac{2}{N} \sum_{i=1}^N \Delta m_i \sin(\omega t_i + \phi),\end{aligned}\quad (\text{A7})$$

where the second term has vanished through the application of Eq. A6. If we square this expression and then take a statistical average, we find

$$\begin{aligned}\langle (\Delta a)^2 \rangle &= \frac{4}{N^2} \sum_{i=1}^N \sum_{j=1}^N \langle \Delta m_i \Delta m_j \rangle \sin(\omega t_i + \phi) \\ &\quad \sin(\omega t_j + \phi) \\ &= \frac{4}{N^2} \sum_{i=1}^N \langle (\Delta m_i)^2 \rangle \sin^2(\omega t_i + \phi) \\ &= \frac{4}{N^2} \sigma^2(m) \sum_{i=1}^N \sin^2(\omega t_i + \phi) \\ &= \frac{2}{N} \sigma^2(m),\end{aligned}\quad (\text{A8})$$

where we have made use of the relations in A1. Writing $\sigma^2(a) = \langle (\Delta a)^2 \rangle$, we have

$$\sigma(a) = \sqrt{\frac{2}{N}} \cdot \sigma(m), \quad (\text{A9})$$

which is the desired relation between photometric and amplitude uncertainties.

We now repeat this analysis for the phase ϕ . From Eq. A6, we have

$$0 = \sum_{i=1}^N [\Delta m_i \cos(\omega t_i + \phi) - m_i \Delta \phi \sin(\omega t_i + \phi)], \quad (\text{A10})$$

which can be rewritten as

$$\Delta \phi \sum_{i=1}^N m_i \sin(\omega t_i + \phi) = \sum_{i=1}^N \Delta m_i \cos(\omega t_i + \phi). \quad (\text{A11})$$

Substituting the expression for a in Eq. A5, we have

$$\frac{N}{2} a \Delta \phi = \sum_{i=1}^N \Delta m_i \cos(\omega t_i + \phi). \quad (\text{A12})$$

Squaring both sides and taking averages, we find that

$$\begin{aligned}\langle (\Delta \phi)^2 \rangle &= \frac{4}{N^2 a^2} \sum_{i=1}^N \sum_{j=1}^N \langle \Delta m_i \Delta m_j \rangle \cos(\omega t_i + \phi) \\ &\quad \cos(\omega t_j + \phi) \\ &= \frac{4}{N^2 a^2} \sigma^2(m) \sum_{i=1}^N \cos^2(\omega t_i + \phi) \\ &= \frac{2}{N} \frac{\sigma^2(m)}{a^2}.\end{aligned}\quad (\text{A13})$$

Setting $\sigma^2(\phi) = \langle (\Delta \phi)^2 \rangle$, we finally arrive at

$$\sigma(\phi) = \sqrt{\frac{2}{N}} \frac{\sigma(m)}{a}, \quad (\text{A14})$$

which is the desired relation between the photometric error, the amplitude of the signal, and the error in the phase determination.

It is common among observers to express ϕ in degrees and to relate the uncertainties in amplitude and phase. The equation then becomes

$$\sigma(\phi) = 57.3 \sigma(a)/a \quad (\text{A15})$$

If the star is multiperiodic, Eq. (A2) should be expanded for the different frequencies. If there are no (or only small) cross terms between the frequencies in the data, the uncertainties can be calculated by applying Eqs. (A9) and (A14) to each pulsation frequency separately.

The expressions derived in this appendix have been thoroughly tested by using the computer program codes of Bevington (1969) for a least-squares fit of an arbitrary function. These programs were applied to a multiperiodic solution of the present data set of 4 CVn. Full agreement with the numbers calculated from the formulae derived above was obtained.

References

- Bevington P.R., 1969, In: Data Reduction and Error Analysis for the Physical Sciences. McGraw-Hill, 204
 Brassard P., Fontaine G., Wesemael F., 1995, ApJS 96, 545
 Breger M., 1990a, A&A 240, 308 (Paper II)

- Breger M., 1990b, *Comm. Asteroseismology (Vienna)* 20, 1
- Breger M., 1993, In: Butler C.J., Elliott I. (eds.) *Stellar Photometry - Current Techniques and Future Developments*. Cambridge University Press, 106
- Breger M., Hiesberger F., 1999, *A&AS* 135, 54 (Paper III)
- Breger M., McNamara B.J., Kerschbaum F., et al., 1990, *A&A* 231, 56 (Paper I)
- Breger M., Stich J., Garrido R., et al., 1993, *A&A* 271, 482
- Breger M., Pamyatnykh A.A., Pikall H., Garrido R., 1999, *A&A* 341, 151
- Dziembowski W., 1977, *Acta Astronomica* 27, 203
- Dziembowski W., 1982, *Acta Astronomica* 32, 147
- Dziembowski W., 1997, In: Provost J., Schieder F.-X. (eds.) *Sounding solar and stellar interiors*. Proc. IAU Symp. 181, Kluwer, Dordrecht, p. 317
- Dziembowski W., Krolikowska M., 1990, *Acta Astronomica* 40, 19
- Fitch W.S., 1980, *Lecture Notes in Physics* 125, 7
- Garrido R., Garcia-Lobo E., Rodriguez E., 1990, *A&A* 234, 262
- Garrido R., Rodriguez E., 1996, *MNRAS* 281, 696
- Jones D.H.P., Haslam C.M., 1966, *The Observatory* 86, 34
- Kuschnig R., Weiss W.W., Gruber R., et al. 1997, *A&A* 328, 544
- Scargle J.D., 1982, *ApJ* 263, 835
- Sperl M., 1998, *Comm. in Asteroseismology (Vienna)* 111, 1
- Watson R.D., 1988, *Ap&SS* 140, 225